

SCIENTIFIC REPORTS



OPEN

A Novel Broadband Band-pass Filter Based on Spoof Surface Plasmon Polaritons

Lei Zhao^{1,2}, Xin Zhang¹, Jun Wang¹, Wenhua Yu¹, Jiandong Li³, Hai Su³ & Xiaopeng Shen^{2,3}

Received: 13 May 2016

Accepted: 10 October 2016

Published: 31 October 2016

In this paper, we present a novel broadband bandpass filter based on spoof surface plasmon polaritons (SSPPs) in the microwave frequency band. The proposed bandpass filter includes three parts: (1) coplanar waveguide (CPW); (2) matching transition; and (3) coupled structure that is an asymmetric coupled filter constructed by five grooved strips. The proposed bandpass filter realizes excellent low loss performance from 7 to 10GHz, in which its insertion loss is around 1.5 dB in the same frequency band. Meanwhile, this filter has a good band stop characteristic from 3 to 7 GHz. A simple but accurate transmission line model was proposed to evaluate the proposed broadband SSPPs filter. The measured data, simulated results and the results obtained from the transmission line model have shown a very good agreement. The proposed planar broadband filter plays an important role for filtering surface plasmon polaritons (SPPs) waves in plasmonic circuits and systems.

Surface plasmon polaritons (SPPs) are highly localized surface waves in the optical frequency region, which propagate parallel to the interface between air and metal and decay exponentially in the vertical direction, since the metal has the similar property to plasma with a negative permittivity^{1,2}. Many researches have demonstrated that the SPPs have the ability to confine light in a subwavelength scale with high intensity, which can be used to tackle the diffraction limit, miniaturize photonic components, and build highly integrated optical components and circuits³⁻⁴. The SPPs have attracted great attentions owing to their huge potential applications in the areas of surface characterization, biomedical sensing, near-field microscopy, nano-photonic and optoelectronic technologies⁵⁻⁷.

When the interested frequency is reduced to terahertz (THz) and microwave bands, the metals behave akin to perfectly electric conductors (PECs), and hence the natural SPPs cannot be invoked on the metal surface. Plasmonic metamaterials have been proposed to produce the so-called spoof SPPs (SSPPs)⁸⁻¹⁵, which can produce highly confined surface electromagnetic (EM) wave at the lower frequencies. An important advantage of this metamaterial is that the dispersion characteristics and spatial confinement of the SSPPs can be controlled by the geometrical parameters of array elements.

As the plasmonic metamaterials are advancing at a rapid pace, they are considered to be a promising candidate in the practical applications¹⁶⁻²². The broadband bandpass filters are key components and play a very important role in various communication and radar systems. A SPPs bandpass filter was designed using a bulky structure with a periodic subwavelength metallic Domino array²³. Recently, efficient filtering effect and ultrathin spoof surface plasmonic waveguides were already reported²⁴⁻³⁴, which show excellent filtering characteristics such as low loss and wideband. However, the existing articles have not given a clear theoretical analysis on the designs. Thereafter, more efforts are still towards to design a bandpass filter with a wide stopband that is highly demanded in practical applications for effective suppression of the undesired noise signal.

In this paper, an ultrathin metallic structure printed on a thin flexible dielectric substrate is proposed to achieve a broadband bandpass filter with a wide bandpass in the microwave frequency band, which is composed of two asymmetrically broken corrugated strips coupled via the grooved strips with an embedded split ring. Two transition sections are also designed to obtain the smooth conversion between the CPW and the SSPPs filter, which can extract the transmitted SSPPs wave from the traditional CPW. The measurement of the SSPPs filter demonstrates a good agreement with the simulated results. Meanwhile, a simple but accurate transmission line

¹Center for Computational Science and Engineering, Jiangsu Normal University, China. ²State Key Laboratory of Millimeter Waves, Southeast University, China. ³Department of Physics, China University of Mining and Technology, China. Correspondence and requests for materials should be addressed to L.Z. (email: leizhao@jnsu.edu.cn) or X.S. (email: xpshen@cumt.edu.cn)

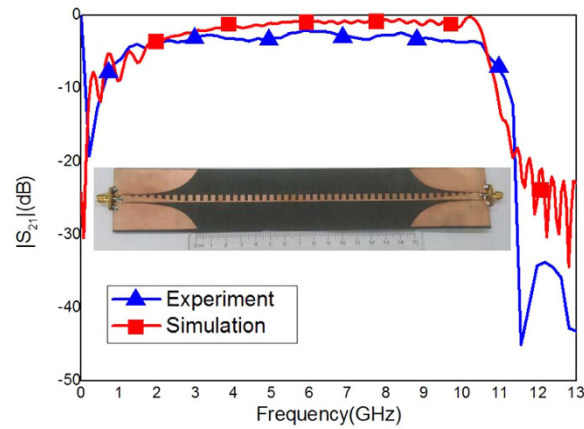


Figure 1. Simulated and measured $|S_{21}|$ of the SSPPs waveguide and the photograph of the fabricated SSPPs waveguide.

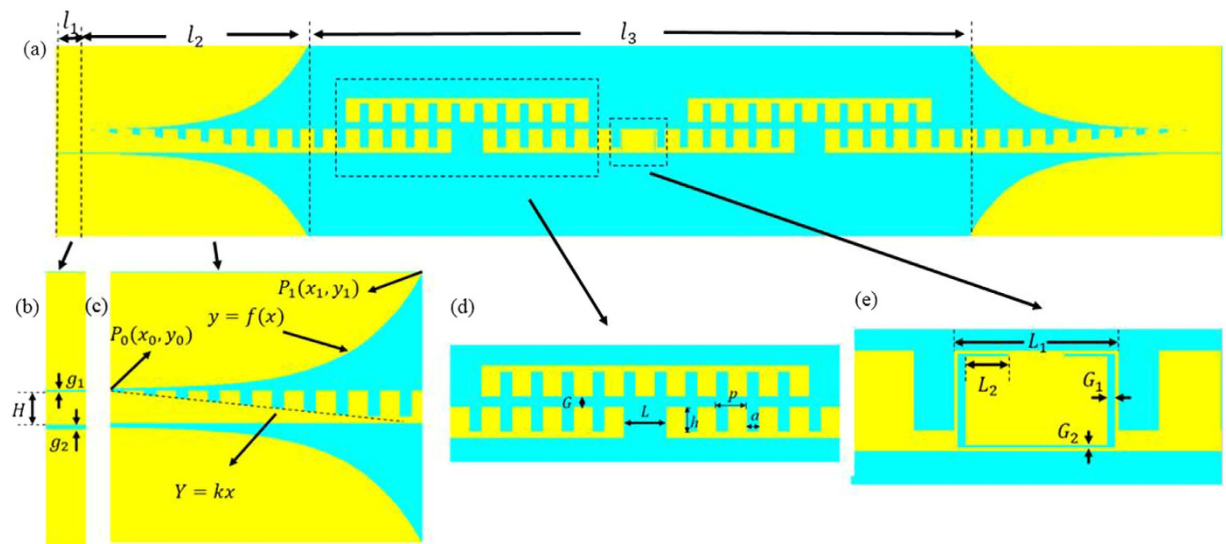


Figure 2. The configuration of SSPPs filter. (a) Top view of the proposed broadband filter, in which $l_1 = 5 \text{ mm}$, $l_2 = 50 \text{ mm}$, and $l_3 = 115 \text{ mm}$. (b) CPW structure, in which $g_1 = 0.13 \text{ mm}$, $g_2 = 0.26 \text{ mm}$ and $H = 5 \text{ mm}$. (c) Matching transition with the gradient grooves and flaring ground, in which $k = 4/45$. (d) Zoomed view of the couple structure, in which $G = 1.8 \text{ mm}$, $L = 7 \text{ mm}$, $h = 4 \text{ mm}$, $p = 5 \text{ mm}$ and $a = 2 \text{ mm}$. (e) Zoomed view of the split ring, in which $L_1 = 8 \text{ mm}$, $L_2 = 2.1 \text{ mm}$, $G_1 = 0.4 \text{ mm}$ and $G_2 = 0.15 \text{ mm}$.

model was first proposed to evaluate the transmission and reflection properties of the proposed filter. Using this compact structure, the proposed SSPPs filter with a low loss and good transmission in the pass band has the absolute advantages in the design of the plasmonic integrated circuits in both microwave and terahertz frequency bands.

Results

As a well-known fact, the SSPPs waveguide has an excellent transmission property, as shown in Fig. 1, whose performance is much better than the traditional microstrip²⁵. Many related works based on this structure have been reported. For example, a planar composite plasmonic waveguide can achieve three or more signals transmission with a good propagation performance²⁶. A broadband and high-efficiency transition is designed to connect a microstrip line to a conformal surface plasmon (CSP) waveguide²⁷. The spoof plasmonic waveguide has much lower propagation loss and longer propagation length compared with the conventional spoof plasmonic waveguide with rectangular grooves²⁸.

Based on this type of SSPPs waveguides, a broadband filter is proposed and optimized in this section, as shown in Fig. 2(a). The yellow and light blue parts in Fig. 2 stand for metal (copper) and flexible thin dielectric substrate, respectively. The thickness of the ultrathin metallic strips is selected to be 0.018 mm and the F4B substrate has a thickness of 0.5 mm. The corrugated metallic strip is launched via two CPWs with a 50 Ω characteristic impedance, and the parameters of this particular structure are accurately retrieved as: $l_1 = 5 \text{ mm}$, $l_2 = 50 \text{ mm}$, and

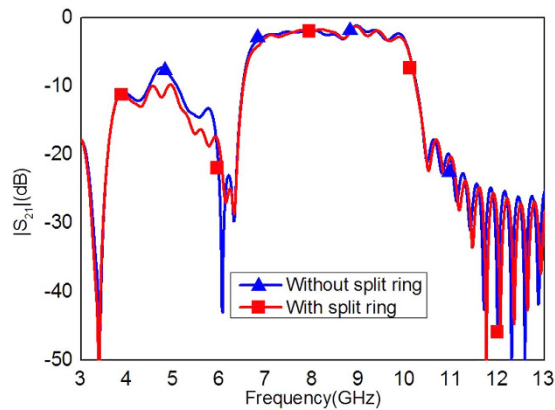


Figure 3. Simulated transmission coefficients $|S_{21}|$ with and without the split ring slot.

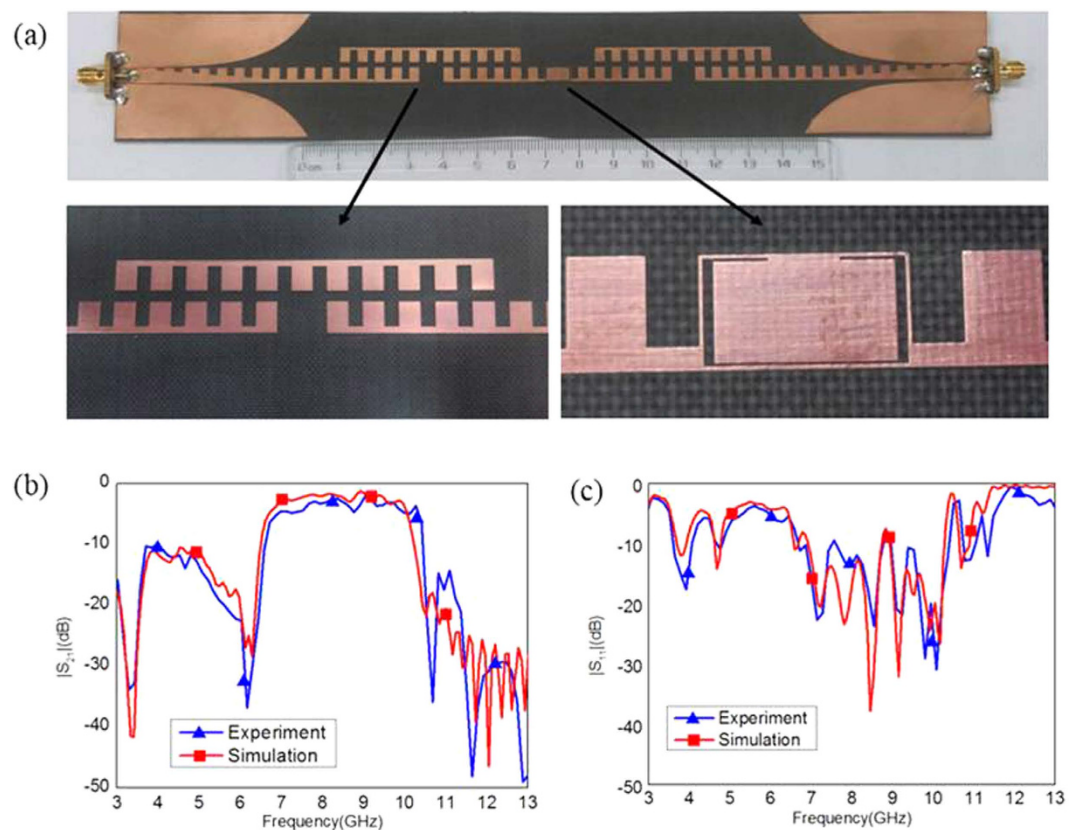


Figure 4. The photograph of the fabricated SSPPs filter and the simulation and measurement result of S-parameters. (a) Photograph of the fabricated SSPPs filter mounted on a flexible dielectric film. (b) The transmission coefficients. (c) The reflection coefficients.

$l_3 = 115 \text{ mm}$. The dash line in Fig. 2(c) is described by using the expression $Y = kx$ ($k = 4/45$). The Vivaldi curve of flaring ground is expressed as:

$$y = C_1 e^{ax} + C_2 (x_1 < x < x_2) \tag{1}$$

where $C_1 = \frac{y_1 - y_0}{e^{ax_1} - e^{ax_0}}$, $C_2 = \frac{y_1 e^{ax_1} - y_0 e^{ax_0}}{e^{ax_1} - e^{ax_0}}$, $a = 0.08$. $P_0(x_0, y_0)$, $P_1(x_1, y_1)$ in Fig. 2(c) are the coordinates of the start and end points of the Vivaldi³⁵. The coupling structure of the proposed filter is illustrated in Fig. 2(d). The period p , the width a , and the depth h of metallic grooves are selected to be 5 mm, 2 mm and 4 mm, respectively; the gap L between the two lower strips is chosen to be 7 mm; and the gap G between the lower and upper strips is chosen to be 1.8 mm. A split ring slot in the middle element of the filter, as shown in Fig. 2(e), is designed to improve the

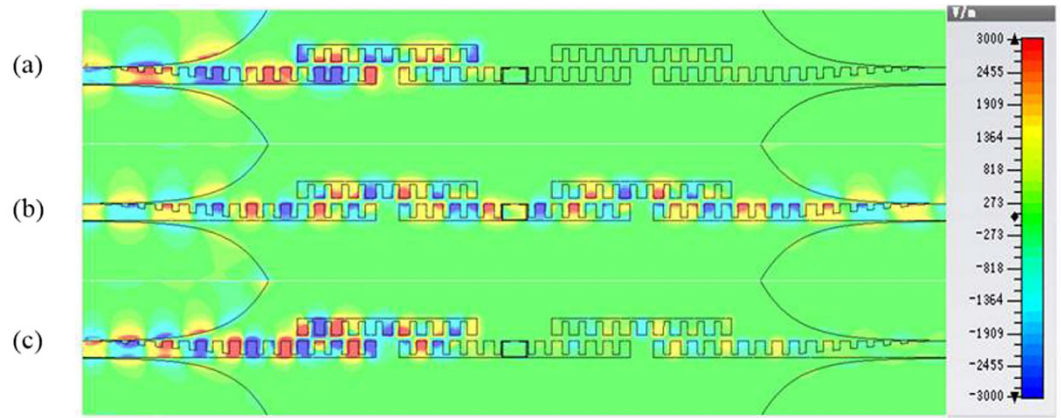


Figure 5. Simulated electric-field distributions on the element side of the proposed filter at different frequencies. (a) $f=6$ GHz. (b) $f=8$ GHz. (c) $f=10$ GHz.

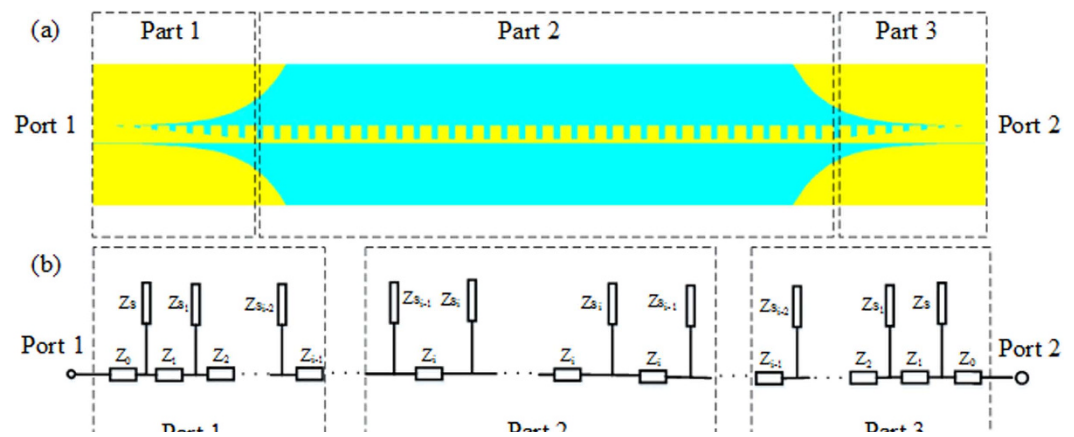


Figure 6. Schematic diagram of the proposed SSPPs waveguide. (a) Transmission line model of the SSPPs waveguide. (b) Equivalent circuit of the SSPPs waveguide.

reflection in the stop band. The dimensions of the split ring slot are optimized to be: the frame length $L_1 = 8$ mm, the shoulder length of the inner patch $L_2 = 2.1$ mm, the side gap $G_1 = 0.4$ mm, and the bottom gap $G_2 = 0.15$ mm. The simulated $|S_{21}|$ of the filter with and without the split ring slot are demonstrated in Fig. 3. It is observed from Fig. 3 that the split ring slot makes the $|S_{21}|$ less than -10 dB at 4.5 GHz.

In the microwave frequency band, the fabricated filter is shown in Fig. 4(a). The measured and simulated S-parameters ($|S_{11}|$ and $|S_{21}|$) are plotted in Fig. 4(b,c). It is evident from Fig. 4 that there exists a good agreement between the simulated results and the measured data. We also notice from Fig. 4 that $|S_{11}|$ is less than -10 dB from 7 to 10 GHz, implying an excellent impedance match of the transition structure from the CPW to the SSPPs filter. It is a fact that the filter only has around 1.5 dB transmission loss in the pass band.

In order to gain insight into the band-pass characteristics of the proposed filter, we present the near-field distributions on the filter surface at different frequencies, as shown in Fig. 5. It is obvious from Fig. 5 that the wave energy cannot propagate through the coupling structure at 6 GHz and 11 GHz since such frequencies are outside the band-pass frequency band. The excellent propagation property at the operating frequency 8 GHz is clearly observed from Fig. 5(b).

Transmission Line Model. The SSPPs waveguide includes a single conductor and seems different from the conventional microwave transmission line. Since the spoof waveguide transmits the wave by coupling between the grooves, its equivalent model can be analyzed by using the transmission line model^{36,37} by considering a very far ground plane at infinity. Based on this definition, we can calculate the capacitors which connect the line to the ground³⁶. This model matches the conventional cases and one can thus use the impedance, scattering and ABCD matrix definitions. Such curved ground design has been used already in another application of using SSP to feed dielectric resonator antennas (DRAs) to achieve isotropic radiation³⁷. In order to validate the proposed transmission line model, we first use it to evaluate the SSPPs waveguide, as shown in Fig. 6. Assuming that the vertical transmission lines have no coupling, the ABCD matrices of the short stub M_i and the open stub N_i ³⁸ are expressed as:

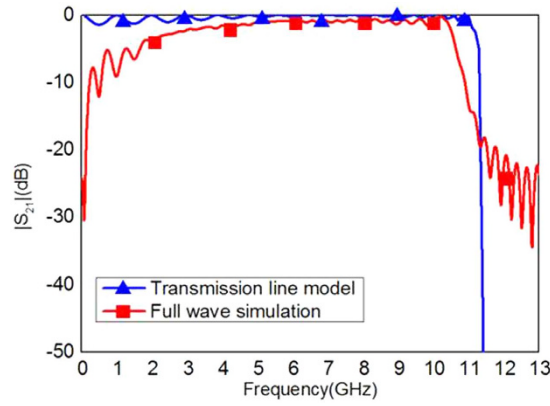


Figure 7. Comparison of $|S_{21}|$ of the proposed SSPPs waveguide obtained from the transmission line model and the full wave simulation.

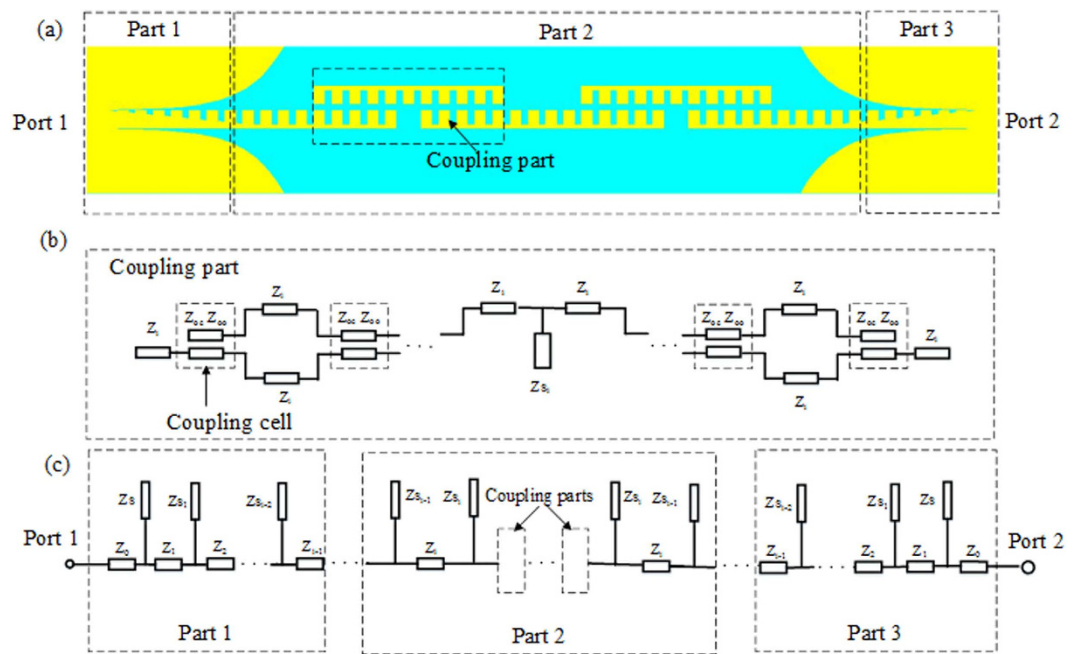


Figure 8. Schematic diagram of the proposed broadband band-pass filter based on the SSPPs waveguide. (a) Model of the broadband band-pass filter. (b) Coupling part of the broadband band-pass filter. (c) Equivalent circuit of the broadband band-pass filter.

$$M_i = \begin{bmatrix} \cos \theta_i & jZ_i \sin \theta_i \\ j \sin \theta_i / Z_i & \cos \theta_i \end{bmatrix}, N_i = \begin{bmatrix} 1 & 0 \\ j \tan \theta_{si} / Z_{si} & 1 \end{bmatrix} \quad (2)$$

where Z_i and Z_{si} are characteristic impedances of the short and open stubs, respectively. θ_i and θ_{si} are the electrical lengths of the short and open stubs, respectively. The ABCD matrix of the entire circuit can be expressed as:

$$M = M_0 \times N_0 \times M_1 \times N_1 \dots M_i \times N_i \dots N_1 \times M_1 \times N_0 \times M_0 \quad (3)$$

Then, using the cascade connection theory of two-port network, S_{11} and S_{21} are obtained as:

$$S_{11} = \frac{A_m + B_m/Z_0 - C_m Z_0 - D_m}{A_m + B_m/Z_0 + C_m Z_0 + D_m} \quad (4)$$

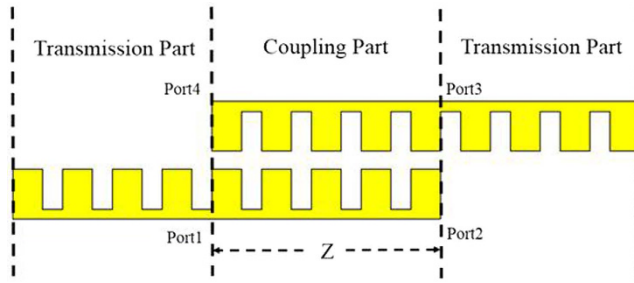


Figure 9. Schematic of the coupling part of the proposed filter.

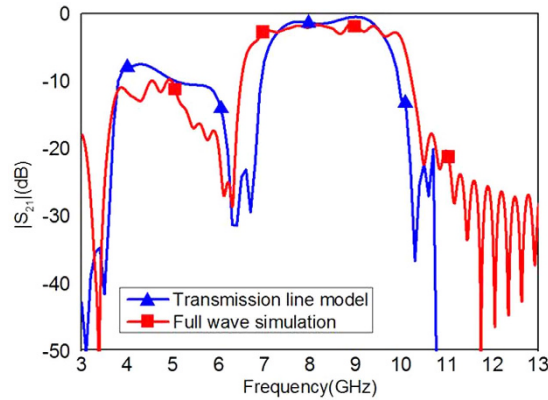


Figure 10. Transmission coefficients of the proposed SSPPs filter obtained by using the transmission line model and the full wave simulation.

$$S_{21} = \frac{2}{A_m + B_m/Z_0 + C_m Z_0 + D_m} \tag{5}$$

where A_m , B_m , C_m , and D_m are the elements of matrix M . The comparison of $|S_{21}|$ obtained by using the full wave simulation and the transmission line model is demonstrated in Fig. 7, and it is evident that they are in a good agreement. The deviation at lower frequencies between the transmission line model and the full wave simulation is caused by the time domain solver used in this paper, which is not accurate at the low frequencies.

The transmission line model for the proposed broadband filter includes the coupling part and equivalent circuit part, as shown in Fig. 8. The detailed structure for the coupling part is demonstrated in Fig. 8(b), in which Z_{oe} and Z_{oo} are the even- and odd-mode characteristic impedances of the coupling unit, respectively. Based on the concept of microwave network, the coupling part can be described by a four-port network³⁹, as shown in Fig. 9. We can get the following relationships for the ports 1, 2, 3, and 4:

$$\begin{bmatrix} b_1 \\ b_2 \\ b_3 \\ b_4 \end{bmatrix} = e^{-j\beta z} \begin{bmatrix} 0 & \cos(\kappa z) & -i \sin(\kappa z) & 0 \\ \cos(\kappa z) & 0 & 0 & -i \sin(\kappa z) \\ -i \sin(\kappa z) & 0 & 0 & \cos(\kappa z) \\ 0 & -i \sin(\kappa z) & \cos(\kappa z) & 0 \end{bmatrix} \begin{bmatrix} a_1 \\ a_2 \\ a_3 \\ a_4 \end{bmatrix} \tag{6}$$

$$\begin{bmatrix} b_2 \\ b_4 \end{bmatrix} = E \begin{bmatrix} a_2 \\ a_4 \end{bmatrix} \tag{7}$$

where κ is the coupling coefficient, and z is the length of coupling cell. The S scattering parameter matrix of the coupling part is

$$S = \begin{bmatrix} \frac{\cos^2(\kappa z)}{e^{2j\beta z} + \sin^2(\kappa z)} & -\frac{2i \sin(\kappa z)e^{j\beta z}}{e^{2j\beta z} + \sin^2(\kappa z)} \\ -\frac{2i \sin(\kappa z)e^{j\beta z}}{e^{2j\beta z} + \sin^2(\kappa z)} & \frac{\cos^2(\kappa z)}{e^{2j\beta z} + \sin^2(\kappa z)} \end{bmatrix} \tag{8}$$

On the base of the equivalent circuit⁴⁰ and Eqs (2–7), we can get the final S_{11} and S_{21} . Figure 10 gives $|S_{21}|$ of the SSPPs filter obtained by using the full wave simulation and equivalent transmission line model, which shows a good agreement between the full wave simulated results and the ones obtained from transmission line model.

Discussion

In this paper, we propose a novel bandpass filter constructed by an ultrathin metallic structure printed on a thin dielectric substrate to generate a broadband property in the microwave frequency band. The filter is composed of two broken corrugated strips and three coupled strips with an embedded ring slot. The traditional CPW is employed to excite the filter and extract the transmitted SSPPs parameters, and two transition sections are designed for smooth conversion between the CPW and the SSPPs waveguide. The performance of the proposed filter has been analyzed using the equivalent transmission line model. The measurement results show that the reflect coefficient is less than -10 dB with the transmission loss around 1.5 dB in the frequency band from 7 to 10 GHz. Such performance makes the proposed structure be a good filter, which may be further used in multi-layer structures in the future for higher integrations.

Methods

With the help of commercial software, CST Microwave Studio, we simulated the dispersion relations, S-parameters and surface fields of the waveguide and filter. As shown in Figs 1(a) and 4(a), the experimental structure is fabricated using a 0.5 mm thin dielectric film with dielectric constant 2.65 and loss tangent 0.001 , respectively. The thickness of metal (copper) film is 0.018 mm. The Agilent Vector Network Analyzer (E5063A) was used to measure the S-parameters (i.e., the reflection coefficients S_{11} and transmission coefficients S_{21}) of the fabricated samples.

References

- Ritchie, R. H. Plasma losses by fast electrons in thin films. *Phys. Rev.* **106**, 874–881 (1957).
- Barnes, W. L., Dereux, A. & Ebbesen, T. W. Surface plasmon subwavelength optics. *Nature* **424**, 824–830 (2003).
- Gramotnev, D. K. & Bozhevolnyi, S. I. Plasmonics beyond the diffraction limit. *Nature Photon.* **4**, 83–91 (2010).
- Fang, N., Lee, H., Sun, C. & Zhang, X. Sub-diffraction-limited optical imaging with a silver superlens. *Science* **308**, 534–537 (2005).
- Ozbay, E. Plasmonics: merging photonics and electronics at nanoscale dimensions. *Science* **311**, 189–193 (2008).
- Kawata, S., Inouye, Y. & Verma, P. Plasmonics for near-field nano-imaging and superlensing. *Nature Photon.* **3**, 388–394 (2009).
- Ozaki, M., Kato, J. & Kawata, S. Surface-Plasmon Holography with White-Light Illumination. *Science* **332**, 218–220 (2011).
- Wang, K. & Mittlemann, D. M. Metal wires for terahertz wave guiding. *Nature* **432**, 376–379 (2004).
- Akalin, T., Treizebre, A. & Bocquet, B. Single-wire transmission lines at terahertz frequencies. *IEEE Trans. Microwave Theory Techn.* **54**, 2762–2767 (2006).
- Harvey, A. F. Periodic and guiding structures at microwave frequencies. *IEEE Trans. Microwave Theory Techn.* **8**, 30–61 (1960).
- Pendry, J. B., Martin-Moreno, L. & Garcia-Vidal, F. J. Mimicking surface plasmons with structured surfaces. *Science* **305**, 847–848 (2004).
- Ulrich, R. & Tacke, M. Submillimeter waveguiding on periodic metal structure. *Appl. Phys. Lett.* **22**, 251–253 (1973).
- Hibbins, A. P., Evans, B. R. & Sambles, J. R. Experimental verification of designer surface plasmons. *Science* **308**, 670–672 (2005).
- Maier, S. A., Andrews, S. R., Martín-Moreno, L. & García-Vidal, F. J. Terahertz surface plasmon-polariton propagation and focusing on periodically corrugated metal wires. *Phys. Rev. Lett.* **97**, 176805 (2006).
- Shen, X., Cui, T. J., Martín-Cano, D. & García-Vidal, F. J. Conformal surface plasmons propagating on ultrathin and flexible films. *Proc. Natl. Acad. Sci.* **110**, 40–45 (2013).
- Pan, B. C., Liao, Z., Zhao, J. & Cui, T. J. Controlling rejections of spoof surface plasmon polaritons using metamaterial particles. *Opt. Exp.* **22**, 13940–13950 (2014).
- Xu, J. J., Zhang, H. C., Zhang, Q. & Cui, T. J. Efficient conversion of surface-plasmon-like modes to spatial radiated modes. *Appl. Phys. Lett.* **106**, 021102 (2015).
- Sun, S. *et al.* Gradient-index meta-surfaces as a bridge linking propagating waves and surface waves. *Nat. Mater.* **11**, 426–431 (2012).
- Yang, Y., Shen, X., Zhao, P., Zhang, H. C. & Cui, T. J. Trapping surface plasmon polaritons on ultrathin corrugated metallic strips in microwave frequencies. *Opt. Exp.* **23**, 7031–7037 (2015).
- Liu, X. *et al.* Planar surface plasmonic waveguide devices based on symmetric corrugated thin film structures. *Opt. Express* **22**, 20107–20116 (2014).
- Zhang, H. C. *et al.* Broadband amplification of spoof surface plasmon polaritons at microwave frequencies. *Laser & Photon. Rev.* **9**, 83–90 (2015).
- Yin, J. Y., Ren, J., Zhang, H. C., Pan, B. C. & Cui, T. J. Broadband Frequency-Selective Spoof Surface Plasmon Polaritons on Ultrathin Metallic Structure. *Sci. Rep.* **5**, 8165 (2015).
- Wu, J. J. *et al.* Bandpass filter based on low frequency spoof surface plasmon polaritons. *Electronics Letters* **48**, 269–270 (2012).
- Gao, X., Zhou, L., Liao, Z., Ma, H. F. & Cui, T. J. An ultra-wideband surface plasmonic filter in microwave frequency. *Appl. Phys. Lett.* **104**, 191603 (2014).
- Ma, H. F., Shen, X., Cheng, Q., Jiang, W. X. & Cui, T. J. Broadband and high efficiency conversion from guided waves to spoof surface plasmon polaritons. *Laser Photonics Rev.* **8**, 146–151 (2014).
- Liu, L. *et al.* Multi-channel composite spoof surface plasmon polaritons propagating along periodically corrugated metallic thin films. *J. Appl. Phys.* **116**, 013501 (2014).
- Liao, Z., Zhao, J., Pan, B. C., Shen, X. P. & Cui, T. J. Broadband transition between microstrip line and conformal surface plasmon waveguide. *Journal of Physics D: Appl. Phys.* **47**, 315103 (2014).
- Zhou, Y. J. & Yang, B. J. Planar spoof plasmonic ultra-wideband filter based on low-loss and compact terahertz waveguide corrugated with dumbbell grooves. *Appl. Opt.* **54**, 4529–4533 (2015).
- Gao, X., Zhou, L. & Cui, T. J. Odd-mode surface plasmon polaritons supported by complementary plasmonic metamaterial. *Sci. Rep.* **5**, 9250 (2015).
- Yin, J. Y., Ren, J., Zhang, H. C., Zhang, Q. & Cui, T. J. Capacitive-coupled Series Spoof Surface Plasmon Polaritons. *Sci. Rep.* **6**, 24605 (2016).
- Zhang, H. C. *et al.* Smaller-loss planar SPP transmission line than conventional microstrip in microwave frequencies. *Sci. Rep.* **6**, 23396 (2016).
- Wu, J. J. *et al.* Open Waveguide Based on Low Frequency Spoof Surface Plasmon Polaritons. *Journal of Electromagnetic Analysis and Applications*. **5**, 58–62 (2013).
- Liu, L. L. *et al.* High-efficiency transition between rectangular waveguide and domino plasmonic waveguide. *Aip Advances*. **5**, 027105 (2015).

34. Liu, L., Li, Z., Xu, B. & Yan, J. A high-efficiency rectangular waveguide to Domino plasmonic waveguide converter in X-band. *3rd Asia-Pacific Conference on Antennas and Propagation*. 974–977 (2014).
35. Zhou, B., Li, H., Zou, X. & Cui, T. J. Broadband and high-gain planar Vivaldi antennas based on inhomogeneous anisotropic zero-index metamaterials. *Prog. Electromagn. Res.* **120**, 235–247 (2011).
36. Kianinejad, A., Chen, Z. N. & Qiu, C. W. Design and modeling of spoof surface plasmon modes-based microwave slow-wave transmission line. *IEEE Trans. Microw. Theory Techn.* **63**(6), 1817–1825 (2015).
37. Kianinejad, A., Chen, Z. N., Zhang, L., Liu, W. & Qiu, C. W. Spoof Plasmon-Based Slow-Wave Excitation of Dielectric Resonator Antennas. *IEEE Trans. Antennas Propagat.* **64**(6), 2094–2099 (2016).
38. Pozar, D. M. In *Microwave Engineering*, Ch. 4, 190 (Wiley, 2005).
39. Haus, H. & Huang, W. Coupled-mode theory. *P. IEEE* **79**, 1505–1518 (1991).
40. Wong, J. S. & Lancaster, M. J. In *Microstrip filters for RF/microwave applications*, Ch. 2, 14–20 (Wiley, 2001).

Acknowledgements

This work was supported in part by the National Science Foundation of China under Grant no. 61372057, in part by the National Science Foundation of China under Grant no. 61372048, and in part by the Open Project of State Key Laboratory of Millimeter Waves under Grant no. K201613.

Author Contributions

L.Z. and X.S. conceived the idea. X.Z. did the simulations and optimization. L.Z., X.Z., J.W. and W.Y. did the theoretical analysis and proposed the transmission line model. X.Z., J.L., H.S. and X.S. performed the measurements. L.Z., X.Z. and W.Y. wrote and edited the manuscript. All authors contributed to the discussion.

Additional Information

Competing financial interests: The authors declare no competing financial interests.

How to cite this article: Zhao, L. *et al.* A Novel Broadband Band-pass Filter Based on Spoof Surface Plasmon Polaritons. *Sci. Rep.* **6**, 36069; doi: 10.1038/srep36069 (2016).

Publisher's note: Springer Nature remains neutral with regard to jurisdictional claims in published maps and institutional affiliations.



This work is licensed under a Creative Commons Attribution 4.0 International License. The images or other third party material in this article are included in the article's Creative Commons license, unless indicated otherwise in the credit line; if the material is not included under the Creative Commons license, users will need to obtain permission from the license holder to reproduce the material. To view a copy of this license, visit <http://creativecommons.org/licenses/by/4.0/>

© The Author(s) 2016